STUDY AND ANALYSIS OF SOLAR AIR HEATER WITH ARTIFICIAL ROUGHENED BROKEN SINUSOIDAL RIBS

Ravindra Shadev, Kundan Kumar, Shivasheesh Kaushik, Vijay Singh Bisht

Abstract— Solar air heaters provides the efficient use of solar energy, which uses the absorber plate to absorb the incoming solar radiations, converting it to thermal energy at its surface, and transferring the thermal energy to the fluid flowing through the collector. It has been observed that the efficiency of the flat plate solar air heater is low because of low convective heat transfer coefficient between the absorber plate and the air flowing over it. The most common and effective way to improve the performance of the solar air heater is to provide artificial roughness elements on the underside of the absorber plate. This work is concerned with the CFD Analysis of Solar Air heater with artificial roughened broken Sinusoidal ribs to predict convective heat transfer properties. Solar air heater is a useful device for extracting heat from solar energy. The Reynolds number (Re) range from 4000 to 20,000for relative roughness height (e/Dh), relative roughness pitch 8 to 14, the angle of curve (α) in the range of 30°–75°, hydraulic diameter 0.0333 meter and gap width g/e=1. The broken sinusoidal roughness on absorber plate of solar air heater with an aspect ratio of 5:1.The roughened absorber plate being heated while the remaining three walls are insulated. Computational fluid dynamics (CFD) simulations were performed using commercially available software ANSYS 15.0The effect of parameters on the heat transfer and friction are compared with the result of smooth duct under similar flow conditions.
Keywords:

Index Terms— Heat Transfer, Artificial Roughness, Broken Sinusoidal Ribs, Ansys !4.5.

1 INTRODUCTION

Energy, the capability to produce motion, force, work, change in shape, change in form etc, is the basic requirement for the survival of human life. Energy defines the Earth's biomes and sustains life. All living things from single-celled microbes to giant blue Whales, exists in a continuous process of consuming, using and storing energy. Kumar et al, [1] investigated the effect of S shaped ribs attached to one heated wall of a rectangular duct of solar air heater ie Absorber plate having roughness parameters as relative roughness pitch (p/e) in the range of 4-16, relative roughness height (e/Dh) in the range of 0.022-0.054, arc angle (α) of 30°-75°, relative roughness width (W/w) of 1-4 and Reynolds number (Re) ranges from 2400-20000. Hans et al, [2] In this experimental investigation, solar air heater duct with aspect ratio 12 roughened with broken arc rib has been investigated. To investigate the influence of roughness parameters of broken arc rib on Nusselt number as well as on friction factor the roughened plate having relative roughness pitch (P/e), relative gap width (g/e), relative gap position (d/w), relative roughness height (e/Dh) and arc angle (α) varying from 4-12, 0.5-2.5, 0.2-0.8, 0.022-0.043 and 15°-75° respectively, have been investigated for Reynolds number range of 2000-16000. The maximum increase in Nusselt number and friction factor over that of continuous arc rib roughened duct was 1.19 and 1.14 times respectively. The corresponding values over that of smooth duct were 2.63 and 2.44 times respectively. Alam et al. [3] investigated the effect of non-circular perforation holes in term of circularity of V-shaped blockages attached to one heated wall of a rectangular duct of solar air heater. Five different hole shapes ranging from circular to square to rectangular in the circularity range of 1–0.6 have been used with varying relative pitch of 4–12, relative blockage height of 0.4–1.0, open area ratio of 5–25% and angle of attack of 30–75° and Reynolds number of flow was varied between 2000 and 20,000. Maximum enhancement in Nusselt number was found to be 350 at angle of attack value of 60° at relative pitch of 8. Yadav and Bhagoria [4] studied the effects of heat transfer and fluid flow characteristics in artificially roughened solar air heater using CFD. The effects of small diameter of transverse wire rib roughness on heat transfer and fluid flow have been investigated. The maximum value of average Nusselt number was found to be 117 for relative roughness pitch of 7.14 and for relative roughness height of 0.042 at a higher Reynolds number, 18,000. The maximum enhancement of average Nusselt number and frictional factor was found to be 2.31and 0.0317 times that of smooth duct for relative roughness pitch of 7.14 and for relative roughness height of 0.042. Kumar et al. [5] carried out an experimental investigation of heat transfer and friction in the flow of air in rectangular ducts having multi v-shaped rib with gap roughness on one broad wall. The investigation encompassed Reynolds number (Re) from 2000 to 20,000, relative gap distance (Gd/Lv) values of 0.24-0.80, relative gap width (g/e) values of 0.5-1.5, relative roughness height (e/D) values of 0.022-0.043, relative roughness pitch (P/e) values of 6-12, relative roughness width ratio (W/w) values of 1-10, angle of attack (α) range of 30°-75°. Lanjewar et al. [6] carried out the experimental investigation of heat transfer and friction factor characteristics of a rectangular duct roughened with W-shaped ribs arranged at an inclination with respect to the flow direction on underside of absorber plate. The duct had a width to height ratio (W/H) of 8.0, relative roughness pitch (p/e) of 10, relative roughness height (e/Dh) of 0.03375 and angle of attack of flow (α) of 30–75° and Reynolds number between 2300–14,000 was used. Maximum ther-

mo-hydraulic performance for W-down ribs was found to be 1.98 while it was 1.81 for W-up ribs in the range of parameters investigated. El-Sebaii et al. [7] carried out an investigation of thermal performance of double pass flat-plate and v-corrugated plate solar air heaters. The results showed that the double pass v-corrugated plate solar air heater is 11-14% compared to double pass flat plate solar air heater. The thermo hydraulic efficiency of double pass v-corrugated plate SAH is 14% higher than that of double pass flat plate solar air heaters. Karmare and Tikekar [8] studied fluid flow and heat transfer in solar air heater by using Computational Fluid Dynamics (CFD). Lower side of collector plate was made rough with metal ribs of circular, square and triangular cross-section, having 60o inclinations to the air flow. The grit rib elements were fixed on the surface in staggered manner to form defined grid. Amongst the different shape and orientations analyzed, the absorber plate of square cross-section rib with 58^0 angle of the attack gave the best possible results. The percentage increase in the heat transfer for 580 rib inclination plate over smooth plate was found to be 30%. Bhushan and Singh [9] made an attempt to review the various methodology used in duct of solar air heaters. An attempt has been made to categorize and review the reported roughness geometries used for creating artificial roughness. Heat transfer coefficient and friction factor correlations developed by various investigators for roughened ducts of solar air heaters have been reported in their study. Kumar and Saini [10] used Computational Fluid Dynamics (CFD) for performance analysis of solar air heater having artificial roughness in the form of thin circular wire in arc shaped geometry. The effect of arc shaped geometry on heat transfer coefficient, friction factor and performance enhancement was investigated covering the range of roughness parameter. Different turbulent models have been used for the analysis and their results are compared. Overall enhancement ratio with a maximum value of 1.7 has been found for the roughness geometry corresponding to relative arc angle (α/90) of 0.333 and relative roughness height (e/D) of 0.0426 for the range of parameters considered. Saini and Verma [11] carried out an experimental study to investigate the effect of roughness and operating parameters on heat transfer and friction factor in a roughened duct provided with dimple-shape roughness geometry.

• Ravindra Shadev, *Research Scholar in Department of Thermal Engineering, UTU (Uttarakhand Technical University) Dehradun, Uttarakhand, India ,PH-9897622826. E-mail: kundankmr79@gmail.com*

• Kundan Kumar, *Research Scholar in Department of Thermal Engineering, UTU (Uttarakhand Technical University) Dehradun, Uttarakhand, India ,PH-9897622826. E-mail: kundankmr79@gmail.com*

• Shivasheesh Kaushik, *AssistantProfessor in Department of MECHANICAL Engineering, AGI (Amarpali Group of Institute) Haldwani, Uttarakhand, India ,PH-9756298215. E-mail: shivasheesh.rachit.kaushik@gmail.com*

• Vijay Singh Bhist, *Assistant Professor in Department of MECHANICAL Engineering, UTU (Uttarakhand Technical University) Dehradun, Uttarakhand, India ,PH-9012233525. E-mail: vsinghbisht5@gmail.com*

Correlations for Nusselt number and friction factor have been developed for solar air heater duct provided such artificial roughness geometry. The maximum value of Nusselt number has been found to be 11,600 corresponding to relative roughness height (e/D) of 0.0379 and relative pitch (p/e) of 10. While minimum value of frictionfactor has been found to be 0.05 corresponding to relative roughness height (e/D) of 0.0289 and relative pitch (p/e) of 0.

2. Governing Equations and Numerical Simulation

2.1 Governing Equation

The behavior of the flow is generally governed by the fundamental principles of the classical mechanics expressing the conservation of mass and momentum. Here the considered steady, incompressible, turbulent flow is modeled by the momentum and continuity equations. The continuity and the momentum equations are as follows.

2.1.1 The Turbulent Modeling

2.1.1.1 Kappa-epsilon model

The K-epsilon model is most commonly used to describe the behavior of turbulent flows. It was proposed by A.N Kolmogrov in 1942, then modified by Harlow and Nakayama and produced K-Epsilon model for turbulence. The Transport Equations for K-Epsilon model are for k, Realizable k-epsilon model and RNG k-epsilon model are some other variants of K-epsilon model. K-epsilon model has solution in some special cases. K-epsilon model is only useful in regions with turbulent, high Reynolds number flow.

2.1.1.2 K – Equation

$$\rho[\bar{u}\frac{\partial k}{\partial x}+\bar{v}\frac{\partial k}{\partial r}]=\frac{\partial}{\partial x}[(\mu_l+\frac{\mu_t}{\sigma_k})\frac{\partial k}{\partial x}]+\frac{1}{r}\frac{\partial}{\partial r}[r(\mu_l+\frac{\mu_t}{\sigma_k})\frac{\partial k}{\partial r}]+\rho g - \rho\varepsilon \quad (2.1)$$

Where, G is the production term and is given by

$$\mu_t[2\{(\frac{\partial \bar{v}}{\partial r})^2+(\frac{\partial \bar{u}}{\partial x})^2+(\frac{\bar{v}}{r})^2\}+(\frac{\partial \bar{u}}{\partial r}+\frac{\partial \bar{v}}{\partial x})^2]$$

The production term represents the transfer of kinetic energy from the mean flow to the turbulent motion through the interaction between the turbulent fluctuations and the mean flow velocity gradients.

2.1.1.3 ε - Equation

$$\rho[\bar{u}\frac{\partial \varepsilon}{\partial x}+\bar{v}\frac{\partial \varepsilon}{\partial r}]=\frac{\partial}{\partial x}[(\mu_l+\frac{\mu_t}{\sigma_\varepsilon})\frac{\partial \varepsilon}{\partial x}]+\frac{1}{r}\frac{\partial}{\partial r}(r\mu_l+\frac{\mu_t}{\sigma_\varepsilon})\frac{\partial \varepsilon}{\partial r}] + C_{S1}G\frac{\varepsilon}{k}-C_{s2}\frac{\varepsilon^2}{k} \quad (2.2)$$

Here C_{s1}, C_{s2}, σ_k and σ_ε are the empirical turbulent constant. The values are considered according to the Launder, et. al. (1974).

2.1.2 PERFORMANCE PARAMETERS

This section describes how heat transfer and pressure drop are characterized. Included are dimensionless groups, equations for heat transfer and efficiency calculations, and equations for making pressure drop calculations. Following the descriptions of the performance parameters, the values as read from the graphs in the research done by Wang, et. al.(1996) for friction factor f and Colburn j-factor vs. Reynolds number.

2.1.3 DIMENSIONLESS GROUPS

Accurate characterisation of the flow friction and heat transfer is very important in rating and sizing heat exchangers. Dimensional groups are used for this characterisation: heat transfer defined with the Colburn factor j and pressure drop defined by friction factor f. Below is a summary of the dimensionless groups used in this project, the equation to calculate it, and a brief description.

2.1.3.1 REYNOLDS NUMBER

The Reynold's number Re represents the ratio of flow inertial forces to viscous forces. The Reynold's number characteristic dimension for this study is the tube collar diameter Dc.

$$\mathrm{Re} = \frac{\rho . U_i . D_h}{\mu} \tag{2.3}$$

2.1.3.2 FRICTION FACTOR F

The Fanning friction factor is the ratio of wall shear stress to the flow kinetic energy. It is related to pressure drop tube heat exchangers as:

$$f = \frac{\Delta p . \frac{D_h}{L_t}}{\frac{1}{2} . \rho . U_i^2} \tag{2.4}$$

Where Lt is length of duct,(m); ρ is air density (Kg/ m^3); Δp is pressure drop (Pa).

3.1.3.2 Nusselt number Nu
The Nusselt number is the ratio of convective conductance h to molecular thermal conductance k/Dh.

$$Nu = \frac{h}{k / D_h} \tag{2.5}$$

The Nusselt number is based on the hydraulic diameter Dh. There are different calculations for this available in the literature. The hydraulic diameter in this study is the ratio of the 4 times the minimum free flow air-side area to the wetted perimeter (ratio of air-side surface area to heat exchanger length), and is given by the following expression (Fornasieri and Mattarolo, 1991).

2.1.3.3 PRANDTL NUMBER PR

The Prandtl number Pr is the ratio of a fluid's momentum diffusivity to thermal diffusivity.

$$\mathrm{Pr} = \frac{\nu}{\alpha} = \frac{\mu C_p}{k} \tag{2.6}$$

`

2.2 PRESSURE DROP

The pressure drop determines the amount of pumping power needed to run a heat exchanger. It is therefore important to characterize the pressure drop for design. This section describes how the pressure drop relates to the pumping power, followed by a description of what causes the pressure drop and finally the pressure drop equations for tube-and-fin heat exchangers are presented as:

$$\Delta p = \frac{L}{D} \frac{\rho V^2}{2} \tag{2.7}$$

Pumping power P is often seen as an important design constraint because the pressure drop in a heat exchanger (along with associated pressure drops in the inlet/outlet headers, nozzles, ducts, etc.) is proportional to the amount of fluid pumping power needed for the heat exchanger to function, as given by the following expression.

3. MATERIAL AND METHEDOLOGY

3.1 SOFTWARE PACKAGE USED:

The available computational fluid dynamics software package FLUENT is used to determine the related problems. FLUENT uses a finite volume method and requires from the user to supply the grid system, physical properties and the boundary conditions. When planning to simulate a problem, basic computation model considerations such as boundary conditions, the size of computational domain, grid topology, two dimensions or three-dimension model, are necessary. For example,

appropriate choice of the grid type can save the set up time and computational expense. Moreover, a careful consideration for the selection of physical models and determination of the solution procedure will produce more efficient results. Dependent on the problem, the geometry can be created and meshed with a careful consideration on the size of the computational domain, and shape, density and smoothness of cells. Once a grid has been fed into FLUENT , check the grids and executes the solution after setting models, boundary conditions, and material properties. FLUENT provides the function for post processing the results and if necessary refined the grids is available and solve again as the above procedure. As described in the objective, the purpose of this study is to investigate numerically the effect of misdistribution in the solar air heater.

The whole analysis is carried out with the help of software "ANSYS Fluent 15.0". ANSYS Fluent 15.0 is computational fluid dynamics (CFD) software package to stimulate fluid flow problems. The three dimensional computational domain modelled using tetrahedral mesh for 3-D models. The complete domain of 3-D duct in all cases have fix element size. Grid independence test was performed to check the validity of the quality of the mesh on the solution. Further refinement did not change the result by more than 0.9% which is taken as the appropriate mesh quality for computation.

3.2 Software Specifications:

3.2.1 Solver:

Default: segregated (solver), implicit (formulation), 3D (space), absolute (velocity formulation), cell based (gradient orientation), superficial velocity

3.2.2 Viscous:

Laminar: laminar Turbulent: k-ε, standard realizable, RNG, standard wall function. Every other setting is default

3.2.3 Material:

Aluminum Default: ρ =2719Kg/m^3, C_p =871 J/KgK, k=202.4 W/mk

3.2.4 Boundary Conditions:

3.2.4.1 Fluid Inlet:

Mass flow rate (Mass flow rate specification method), Total temperature = 300K, Operating pressure = 101325 Pa, Direction vector (Direction specification method), Absolute (Reference frame), Z- component of flow direction = 1, Y-component of flow direction = 0, Intensity and hydraulic diameter (Turbulence specification method), Turbulence intensity = 5%.

3.2.4.2 Outlet Wall:

Default: pressure-outlet
Thermal: Temperature (Thermal conditions),Heat flux on absorber plate = 1000 W/m2 Wall thickness = 0m, Heat generation rate 0 w/m^3 , Material name : aluminum , Momentum: Stationary wall (Wall motion), No slip (shear condition), Roughness height = 0m, Roughness constant = 0.5

3.2.5 Residual monitors:

Print and Plot (Options), Default: Convergence criterion; Continuity = .001, X-velocity = 0.001, Y-velocity = 0.001, Energy = 1e-06, k=0.001, H=0.001. Scale (Normalization)

3.2.6 Solution initialization:

Default: Relative to cell zone (Reference frame), Initial values: Gauge pressure = 0Pa, X-velocity = 0m/s, Y-velocity = 0m/s, Turbulent kinetic energy 1.39m^2/s^2, Turbulent dissipation rate=1.73 m^2/s^3, Temperature = 300K

3.2.7 Run calculation:

Number of iterations = 500

3.3 Methodology

The methodology of the present study can be divided into four stages of process flow which are geometry modeling, preprocessing, processing and post-processing. Various steps in adopted methods are:

- Developed the model in SOLIDWORKS.
- Validation of present work with previous research.
- Calculation of heat transfer parameters.
- Run program to obtain the plots with different parameters.
- Plotting & analysis of obtained plots.
- Optimization of the system.

3.4 Simulation of flow through solar air heater:

For the CFD analysis of solar air heater first the fluid domain was designed using Solid works. The boundary conditions applied to the channel, the assumptions made, the equations used, the results obtained after calculation and then the results were analysed.

3.5 Absorber Plate geometry:

Modeling of 3D model of artificially roughened absorber plate with Broken S shapes ribs is done In Ansys Workbench Fluent

15.0. Then ICEM-CFD was used as preprocessor for the purpose of volumetric meshing. Plate material type was set as aluminum.

Figure 3.1: Pictorial view of absorber plate

Table Number 3.1: Model Geometrical details

Geometric Parameter		
Geometric parameter	Symbol	Value
Entrance length of duct, mm	L	280
Width of duct, mm	W	100
Depth of duct, mm	H	20
Hydraulic diameter, mm	Dh	33.33

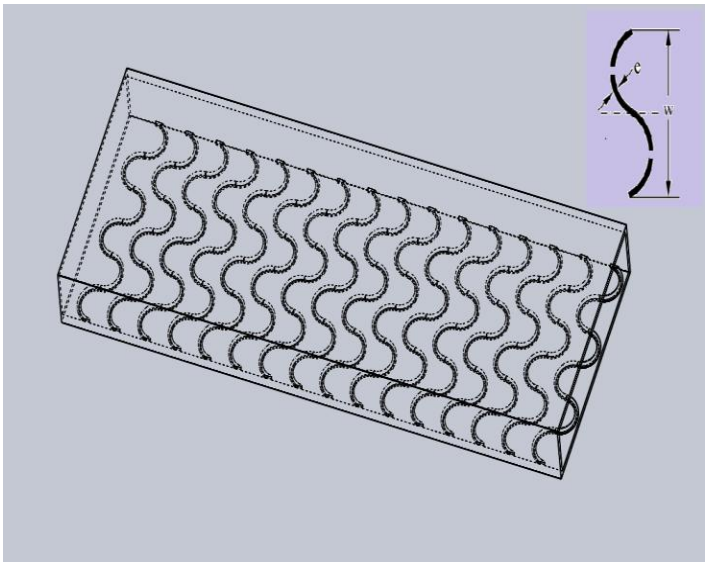

Figure 3.2: Dimensional view of absorber plate

3.6 MESHING VIEW OF THE ABSORBER PLATE

After creating the geometry, meshing was done in which a uniform tetrahedral mesh was selected for the entire domain and a uniform mesh is formed over the entire model.

Table Number 3.2: Range of parameter

S.N.	Parameters	Range
1.	Reynolds number (Re)	3000 to 18000 (6 values)
2.	Duct aspect ratio (W/H)	5 (Fixed)
3.	Relative roughness height (e/Dh)	0.022 to 0.054 (4 values)
4.	Relative roughness pitch (p/e)	4-16 (4 values)
5.	Relative roughness width (W/w)	1-4 (4 values)

Table Number 3.3: Operating parameters used.

Operating parameters		
Location	Boundary condition	Value
Inlet	Velocity inlet	1.32- 7.92m/s
Outlet	Pressure outlet (gauge)	0
Absorber plate	Constant heat flux	1000 W/m2
Other walls	Insulated	-

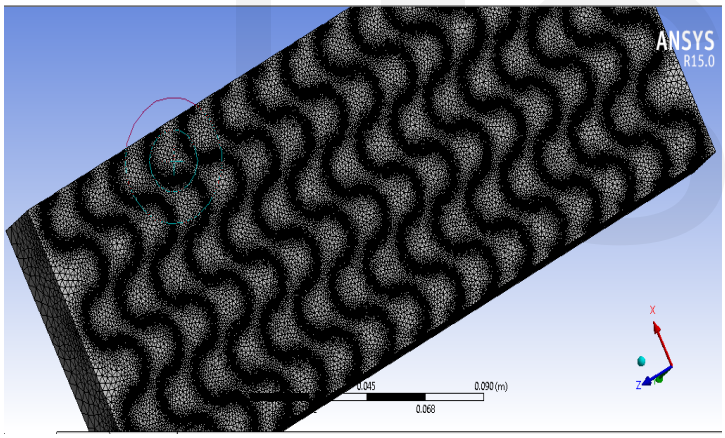

Figure 3.3: Meshing view of the absorber plat

4. Result and Discussion

4.1 Validation of system:

In present work solar air heater is analysed for performance enhancement. Simple solar air heater and Solar air heater with triangular shape geometry inside the tube is analysed. CFD analysis of both design carried out in ANSYS Fluent 15.

4.1.1 Grid independence test:

For selection of mesh element count different no of mesh element size 265131, 871997, 1508485 and 2080414 are performed on smooth duct for nusselt no. at different Reynolds no. the value of Nusslt no. increases initially but after mesh element 1508485 the value of nusselt no. is constant so for calculation of nusselt number for smooth duct 1508485 mesh element is

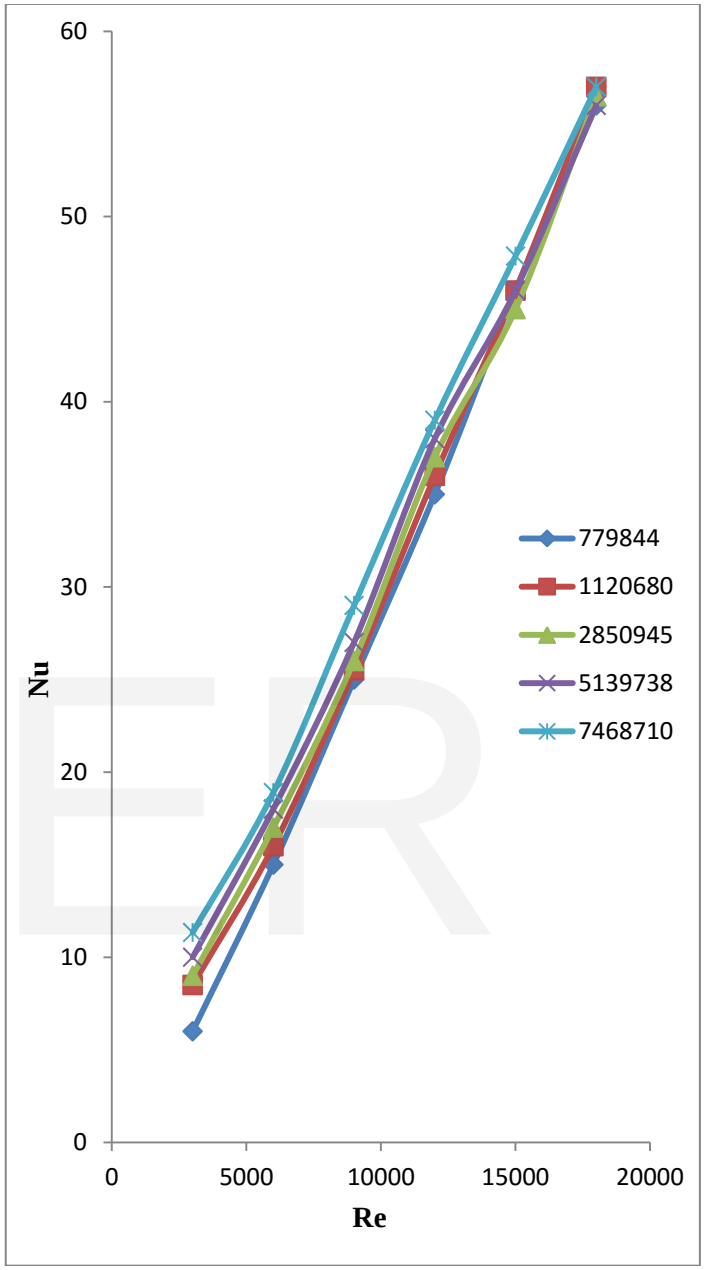

Figure 4.1: Grid independence test

4.2 Validation graphs for uncertainty of model

Validation of model with smooth duct with dittus boelter equation and different turbulence model which are used and compared to see the difference for suitable results. Turbulence model are selected based on the value of Nusselt number with respect to Reynolds number for both design. K-ε model standard and K-ε model RNG, are used to verify the results. The Nusselt number obtained using Dittus-Boelter eq. for both design As the result of different turbulence models compare with dittus-Boelter K-ε turbulence RNG model is gives better result its near to study the present work.

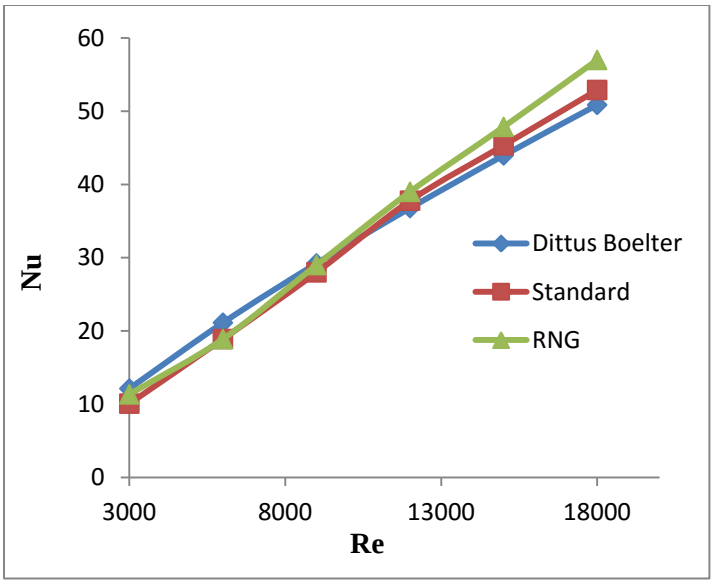

Figure 4.2: Nusselt No. vs Reynold No. graph for smooth plate

4.2.1 Friction factor vs Reynolds No. graph for smooth plateF

For smooth plate value of friction factor decreases as value of Reynolds No increases. In graph shown in Fig:_ shows the friction factor variation using turbulent model K-e RNG and Turbulent model Standard and compared with the values obtained from Modified Blasius Equation.

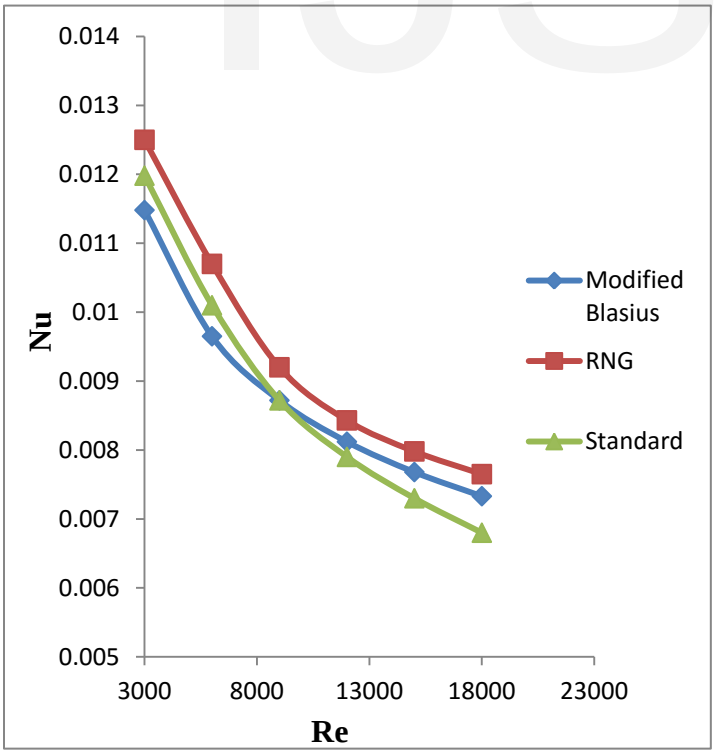

Figure 4.3: Friction factor vs Reynold No. graph for smooth plate

4.3 Effect of relative roughness pitch (p/e)

Figures 13 and 14 shows the effect of relative roughness pitch (p/e) on Nusselt number and friction factor. These graphs had been plotted for Nusselt number and friction factor as the function of Reynolds number for fixed values of the other roughness parameters. It is observed from Figures 13 and 14; that the value of Nusselt number and friction factor attains an optimum value corresponding to a relative roughness pitch (p/e) value of 8 and then a significant decrease in the values of Nusselt number and friction factor values on either side of this relative roughness pitch (p/e) value of 8 had been observed. This deviation occurs due to the reattachment of free shearing layer on downstream the rib and development of the boundary layer up to the next rib which does not occur for lower p/e values.

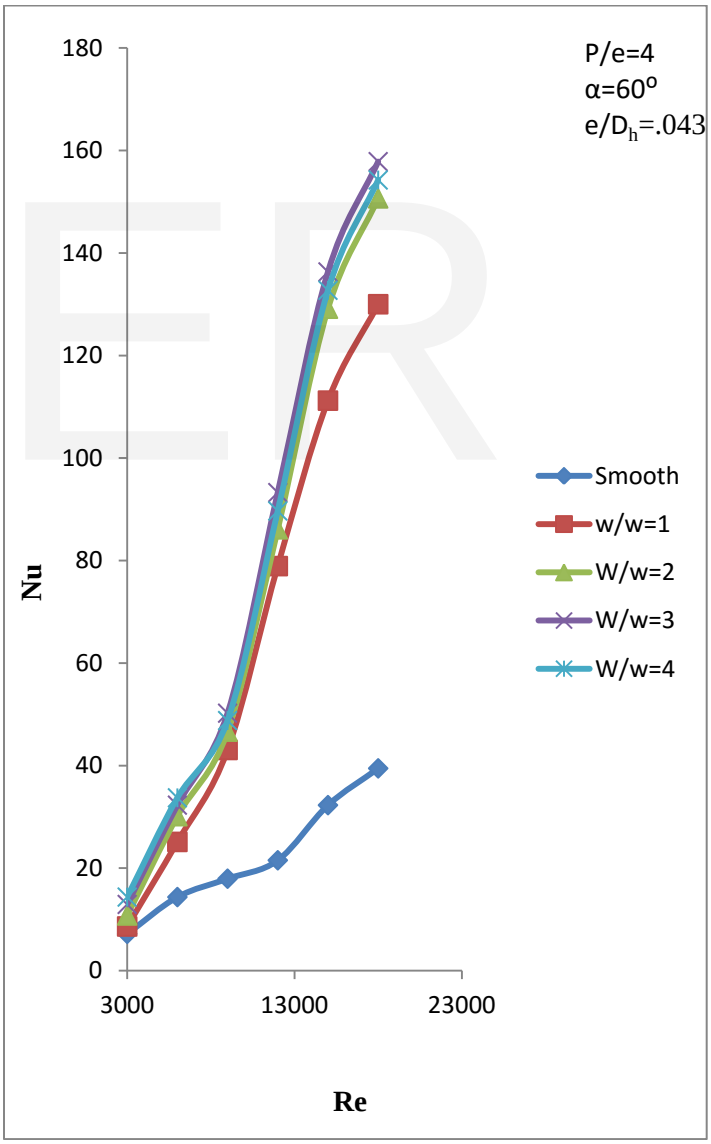

Figure 4.4: Nusselt No vs Reynolds No graph for relative roughness pitch (p/e) of 4

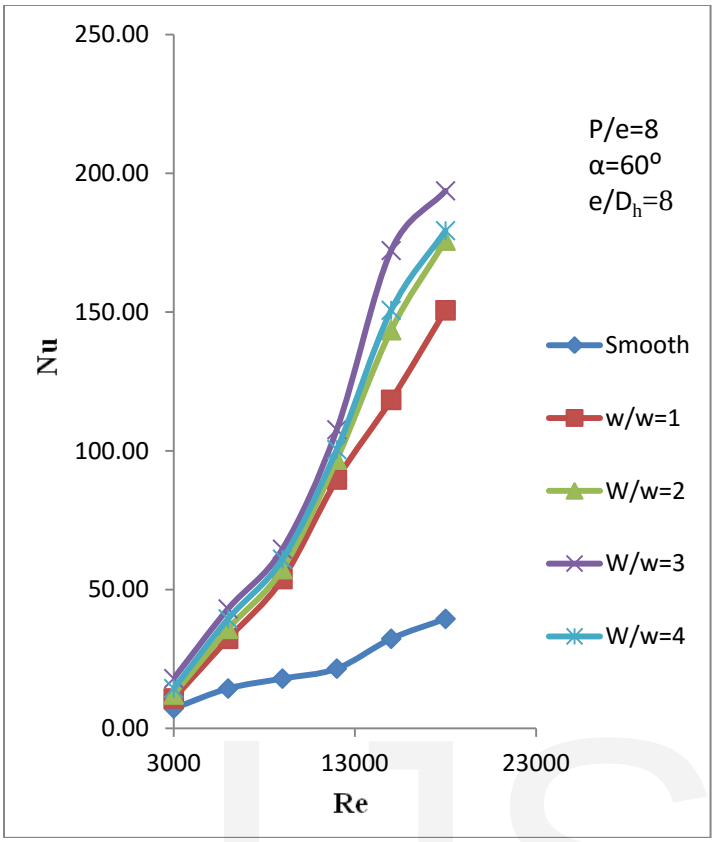

Figure 4.5: Nusselt No vs Reynolds No graph for relative roughness pitch (p/e) of 8

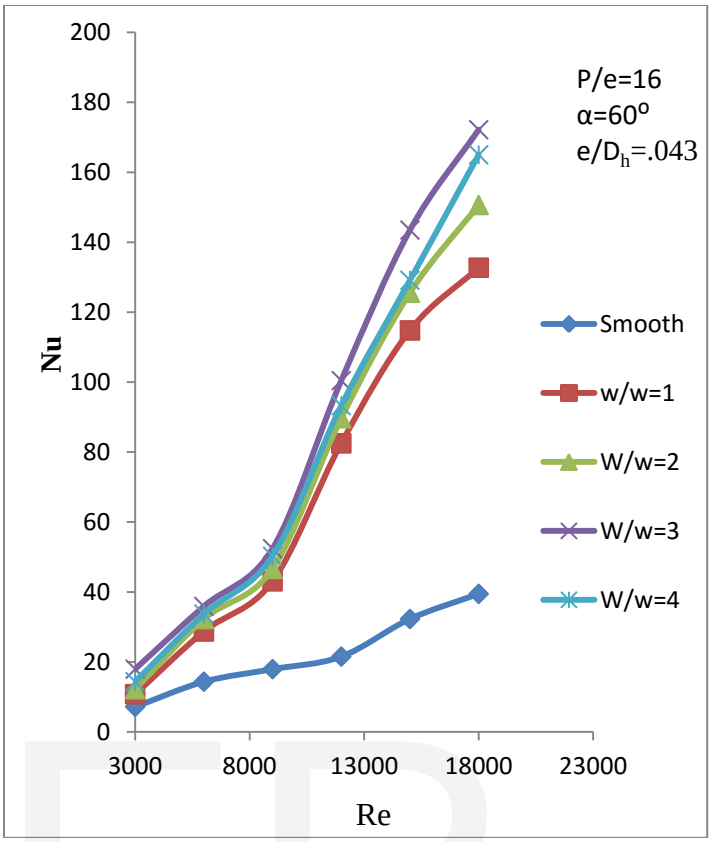

Figure 4.7: Nusselt No vs Reynolds No graph for relative roughness pitch (p/e) of 16

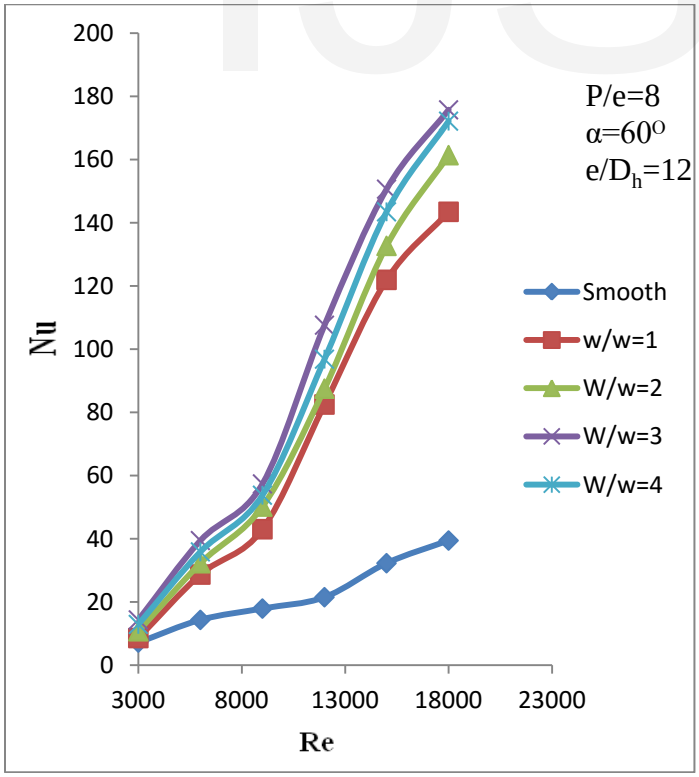

Figure 4.6: Nusselt No vs Reynolds No graph for relative roughness pitch (p/e) of 12

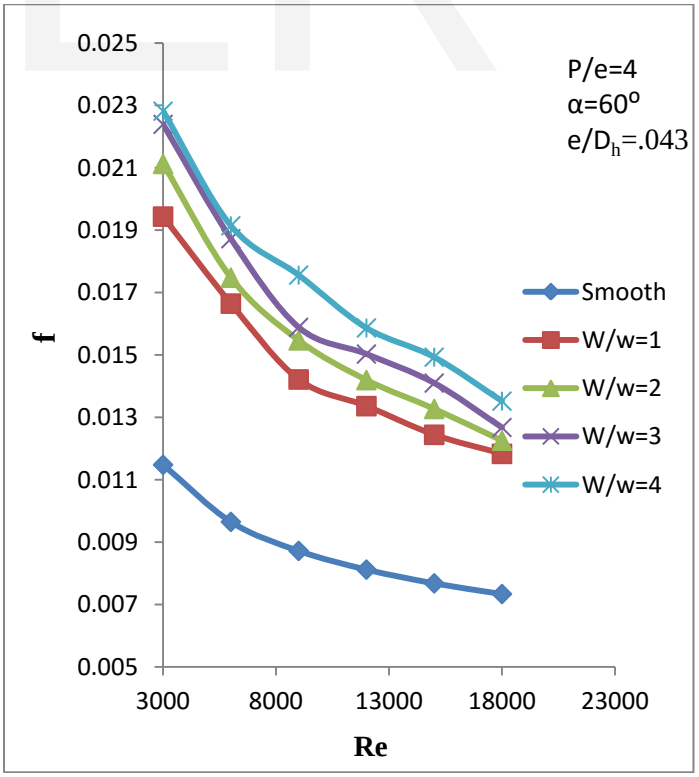

Figure 4.8: Variation of friction factor with Re No at relative roughness pitch (p/e) of 4

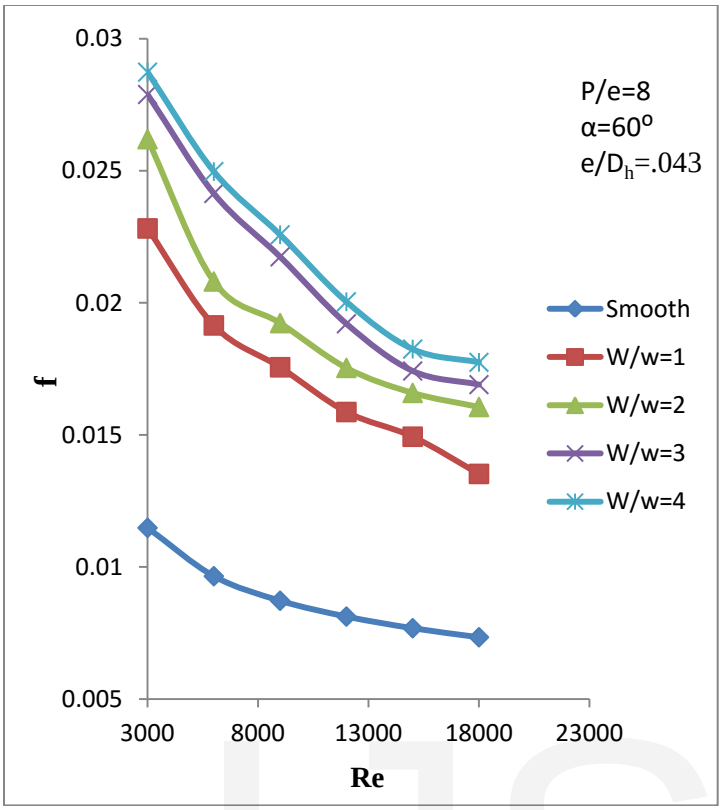

Figure 4.9: Variation of friction factor with Re No at relative roughness pitch (p/e) of 8

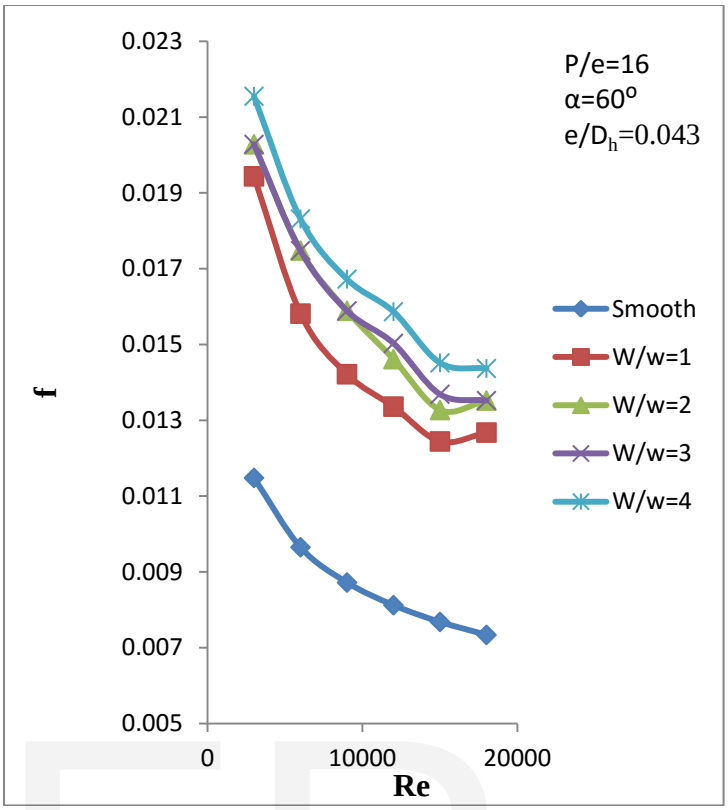

Figure 4.11: Variation of friction factor with Re No. at relative roughness pitch (p/e) of 16

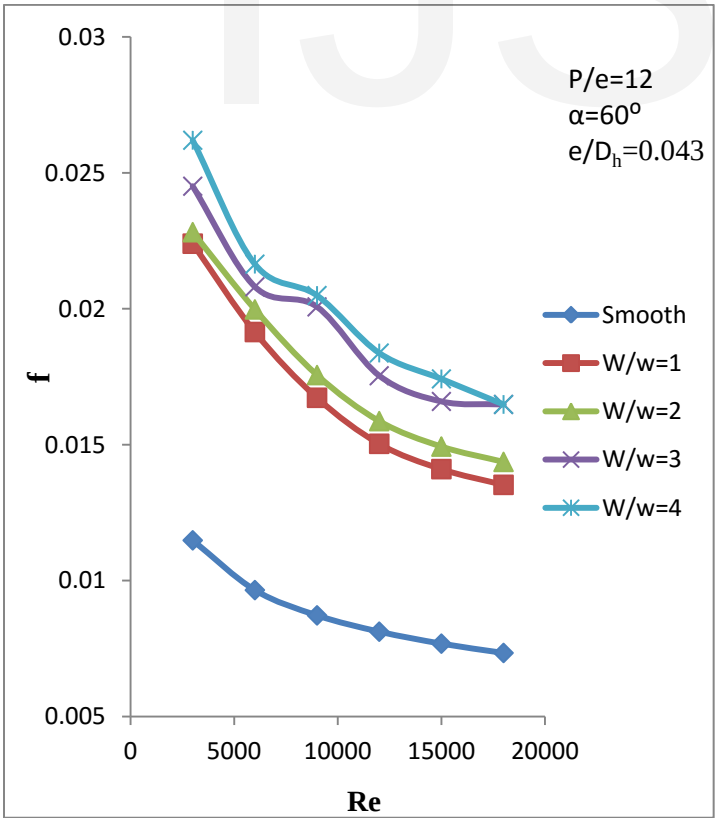

Figure 4.10: Variation of friction factor with Re No at relative roughness pitch (p/e) of 12

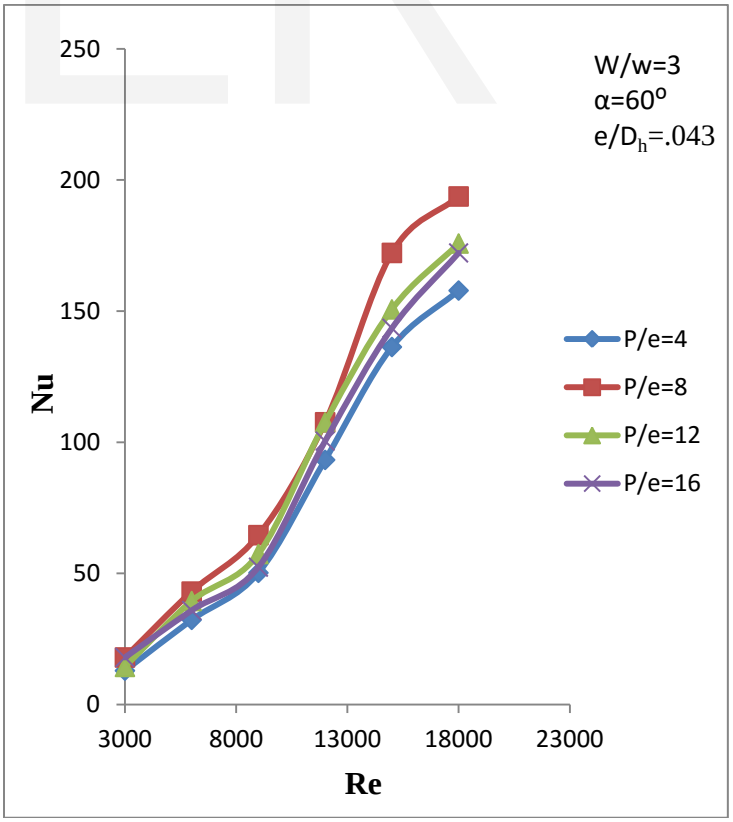

Figure 4.12: Variation of Nusselt number with Reynolds number for different values of p/e at fixed values of parameters.

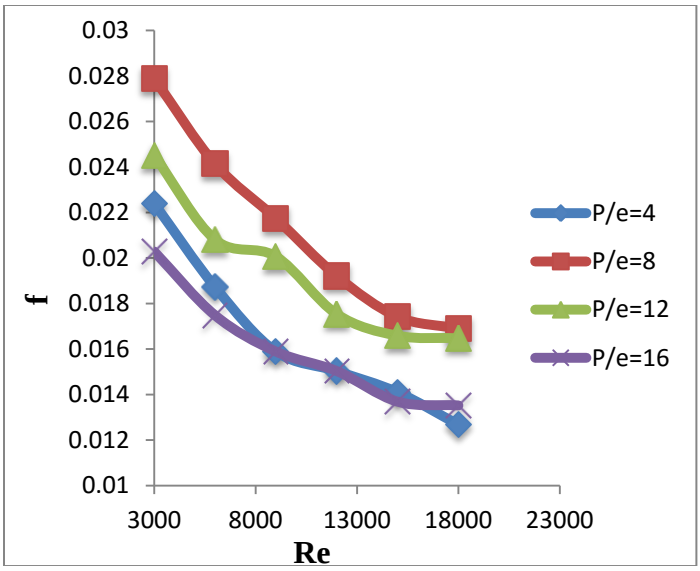

Figure 4.13: Variation of friction factor with Re No for different values of p/e at fixed values of other parameters

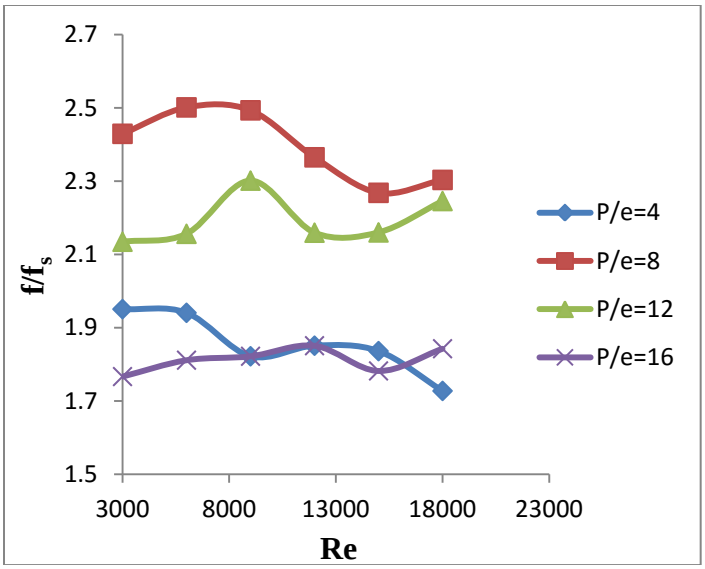

Figure 4.15: Friction factor for Rough Surface vs Friction factor for smooth surface

4.4 Enhanced Nusselt No:

This is the ratio of Nusselt No. for Rough Surface and Nusselt No. for smooth surface. This shows the enhancement in Nusselt No. after creating artificial roughness as compare to smooth surface. By graph in fig: we could find that at relative pitch heigh (P/e) of 8 value of Nusselt No. is maximum.

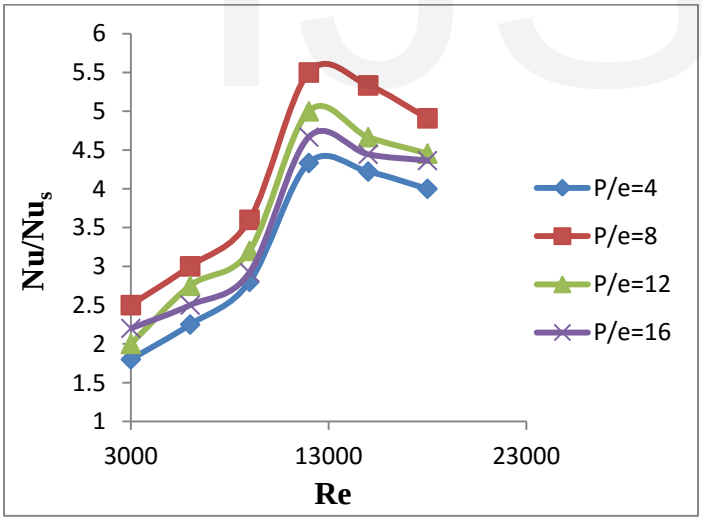

Figure 4.14: Nusselt No. for Rough Surface vs Nusselt No. for smooth surface

4.5 Enhanced Friction factor

This is the ratio of Friction factor for Rough Surface and Friction factor for smooth surface. This shows the enhancement in friction factor after creating artificial roughness as compare to smooth surface. By graph in fig: we fing that for relative pitch heigh (P/e) of 8 value of friction factor is maximum.

4.6 Thermohydraulic performance comparison

Thermohydraulic performance of Broken S shaped ribs is evaluated in terms of thermohydraulic performance parameter which is defined as

$$\eta = Nu/Nus/(f/fs)0.33 \quad (4.1)$$

Thermohydraulic performance parameter Broken S shaped ribs gap has been evaluated with considering the optimum values of roughness geometry parameters for each geometry. For evaluating thermohydraulic performance parameter of broken arc geometry, maximum value of Nusselt number and friction factor obtained experimentally have been considered.

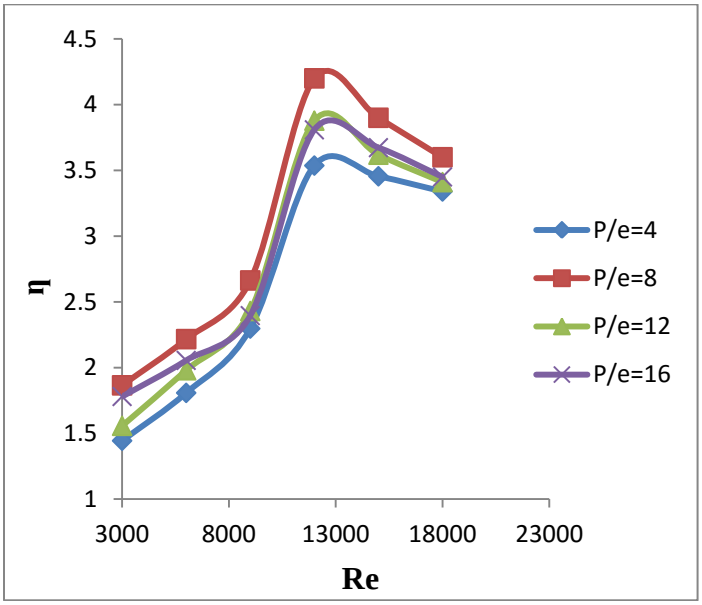

Figure 4.16: Thermohydraulic factor vs Reynolds No

CONCLUSION

In this CFD analysis, operation performed on Ansys Fluent 15.0 the effect of arc shape ribs arranged in Broken 'S' shaped pattern on one of the broad wall of solar air heater duct has been investigated. The effect of the relative roughness width (W/w), relative roughness pitches (p/e) and relative roughness height (e/Dh) on heat transfer (Nusselt number) and friction factor has been analyzed. Based on this investigation the following conclusions were made.

i) Significant enhancement in heat transfer and friction factor can be achieved by creating the artificial roughness in the solar air heater as compared to the smooth duct.

ii) Reynolds number has strong impact on both Nusselt number and friction factor as Nusselt number increases while friction factor decreases with increase in Reynolds number.

iii) Maximum enhancement in heat transfer (Nu) and friction factor (f) occurs for relative arc angle (α/90) value of 0.6667 and relative roughness height (e/Dh) value of 0.043, and it decreases on either side of these values.

iv)Maximum enhancement in heat transfer (Nu) occurs for relative roughness width (W/w) value of 3 while the friction factor goes on increasing with further rise in value of relative roughness width (W/w).

REFERENCES

[1] KHUSHMEET KUMAR, D.R. PRAJAPATI, SUSHANT SAMIR, INVESTIGATION ON HEAT TRANSFER AND FRICTION FACTOR CORRELATIONS DEVELOPMENT FOR SOLAR AIR HEATER DUCT ARTIFICIALLY ROUGHENED WITH 'S' SHAPE RIBS

[2] R.S. Gill, V.S. Hans, J.S. Saini, Sukhmeet Singh, Investigation on performance enhancement due to staggered piece in a broken arc rib roughened solar air heater duct, Renewable Energy (2016), doi: 10.1016/j.renene.2016.12.002

[3] Yadav and Bhagoria " A CFD base heat transfer and fluid flow analysis of a solar air heater provided with circular transverse wire rib roughness on the absorber plate."Renewable energy (2013).

[4] A review on Solar Air Heater using various artificial roughness geometries Ankit C.Khandelwal, 2Samir A.Dhatkar, 3A.B.Kanas-Pat

[5] Deep Singh Thakur, Mohd. Kaleem Khan, Manabendra Pathak, Performance Evaluation of Solar Air Heater With Novel Hyperbolic Rib Geometry, Renewable Energy (2016), doi:10.1016/j.renene.2016.12.092

[6] Jaurker, A.R. Saini, J.S. and Gandhi, B.K., (2006). Heat transfer and friction characteristics of rectangular solar air heater duct using rib-grooved artificial roughness, Solar Energy, 80, pp. 895 – 907.

[7] Karmare, S.V. and Tikekar, A.N., (2007). Heat transfer and friction factor correlation for artificially roughened duct with metal grit ribs, Int. Journal of Heat Mass Transfer, 50, pp. 4342 – 4351.

[8] Karwa, R. Solanki, S.C. and Saini, J.S., (1999) Heat transfer coefficient and friction factor correlations for\ the transitional flow regimes in rib-roughened rectangular duct, Int. Journal of Heat Mass Transfer

[9] T. Alam, R.P. Saini, J.S. Saini, Use of turbulators for heat transfer augmentation in an air 15 duct – a review, Renewable Energy, 62 (2014), pp. 689–715

[10] Aharwal, Gandhi and saini "Heat transfer and friction characteristics of solar air heater ducts having integral inclined discrete ribs on absorber plate" Heat and mass transfer (2009).

[11] Langewar , Bhagoria and Agrawal "Review of development of artificial roughness in solar air heater and performance evaluation of different orientations for double arc rib roughness"

[12] Singh A.P., Varun, Siddhartha, (2014), "Effect of artificial roughness on heat transfer and friction characteristics having multiple arc shaped roughness element on the absorber plate", Solar Energy, Vol. 105, pp. 479 – 493.